

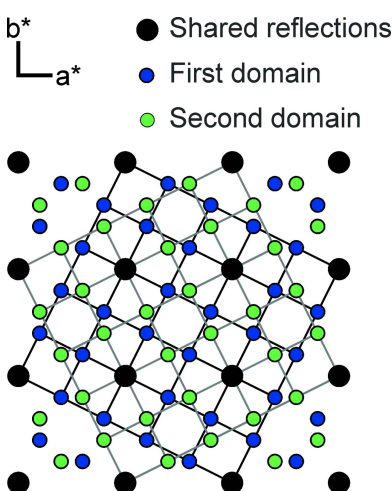
Received 12 April 2022
Accepted 5 May 2022

Edited by M. Weil, Vienna University of
Technology, Austria

Keywords: crystal structure; telluride; rare earth
metal; superstructure; twinning.

CCDC reference: 2170854

Supporting information: this article has
supporting information at journals.iucr.org/e



OPEN ACCESS

Published under a CC BY 4.0 licence

LaTe_{1.9}: a tenfold superstructure of the ZrSSi type

Hagen Poddig and Thomas Doert*

Faculty of Chemistry and Food Chemistry, TU Dresden, D-01062 Dresden, Germany. *Correspondence e-mail:
thomas.doert@tu-dresden.de

Single crystals of LaTe_{1.9} (lanthanum telluride) have been obtained by chemical transport reactions with iodine as transport agent. LaTe_{1.9} adopts the CeSe_{1.9} structure type and crystallizes in the space group $P4_2/n$ with lattice parameters $a = 10.1072(3)$ Å and $c = 18.2874(6)$ Å. The crystal structure comprises an alternating stacking of puckered [LaTe] slabs and planar [Te] layers along [001]. The planar [Te] layer is dominated by dumbbell-shaped Te₂²⁻ anions along an isolated Te²⁻ anion and a vacancy. The Te₂²⁻ anions form an eight-membered ring enclosing the vacancy in the centre.

1. Chemical context

Chalcogenides $REX_{2-\delta}$ ($RE = Y, La-Nd, Sm, Gd-Lu; X = S, Se, Te$) of trivalent rare-earth metals comprise a large structural variety in a small compositional range $0 \leq \delta \leq 0.2$. This variety can mainly be attributed to the amount of vacancies as this strongly affects the final structural motif (Doert & Müller, 2016). All crystal structures share a common motif of alternating [REX] and planar [X] layers, related to their common aristotype, the structure of ZrSSi. Here, the same stacking arrangement is observed with a puckered [ZrS] slab and a planar [Si] layer, where an idealized square-planar [Si] layer is realized (Onken *et al.*, 1964; Klein Haneveld & Jellinek, 1964). The chalcogenides, however, do not form a square-planar arrangement for electronic reasons, which can be understood by their charge-balanced formula: considering trivalent rare-earth metal cations only, the puckered [REX] slab bears a single positive charge per formula unit, which needs to be compensated by atoms of the planar [X] layer. This is achieved by forming dinuclear X_2^{2-} anions in the stoichiometric dichalcogenides REX_2 . The formation of such dumbbell-shaped anions results in a distortion from the ideal square-planar layer. Reducing the chalcogenide content results in the formation of vacancies inside the planar [X] layer, which in turn forces a reaction of the remaining atoms to balance the missing charge. Consequently, an isolated X^{2-} anion per vacancy is formed to maintain a charge-balanced motif, adding two new constituting fragments to the planar layer. As vacancies are not randomly distributed within the layer, commensurate and incommensurately modulated superstructures are found (Doert & Müller, 2016). The structural chemistry of the corresponding sulfides and selenides has been thoroughly investigated, revealing several crystal structures that are observed for both chalcogens. The tellurides, however, do not always match the structures of their sulfur and selenium congeners, as shown for LaTe₂ (Stöwe, 2000a), CeTe₂ (Stöwe, 2000b) and PrTe₂ (Stöwe, 2000c). Discrepancies are also observed for the Te-deficient compound NdTe_{1.89(1)} (Stöwe,

2001). However, the CeSe_{1.9} type (Plambeck-Fischer *et al.*, 1989) with a $\sqrt{5} \times \sqrt{5} \times 2$ supercell of the basic ZrSSi structure seems common to sulfides, selenides and tellurides. CeTe_{1.9} was found to adopt this superstructure in space group *P4*₂/*n* (No. 86) (Ijjaali & Ibers, 2006). The general motif of alternating stacks of [RETe] slabs and planar [Te] layers is preserved in this structure, the planar [Te] layer comprise four Te²⁻ anions surrounding a vacancy, resembling an eight-membered Te ring with alternating long and short distances. Four of these Te rings surround an isolated Te²⁻ anion in a pinwheel-like arrangement. Rationalizing this motif yields ten negative charges due to four Te₂²⁻ and a single Te²⁻ anion, balancing ten positive charges of each [RETe] layer. Here we report on the isotopic compound LaTe_{1.9}, for which no structural characterization has been published yet.

2. Structural commentary

LaTe_{1.9} crystallizes in space group *P4*₂/*n* (No. 86) in the CeSe_{1.9} structure type (Plambeck-Fischer *et al.*, 1989) with $a = 10.1072(3)$ Å and $c = 18.2874(6)$ Å, corresponding to a $\sqrt{5} \times \sqrt{5} \times 2$ superstructure of the basic ZrSSi unit cell. As indicated above, two stacks of the basic arrangement are present in the structure of LaTe_{1.9} as the Te-deficient planar [Te] layers are shifted by an *n*-glide against each other (Fig. 1). The La atoms are coordinated by eight Te atoms (La2), respectively nine Te atoms (La1, La3) forming a bicapped, respectively a tricapped trigonal prism. The La–Te distances within the slabs range from 3.2637(2) to 3.3594(2) Å and

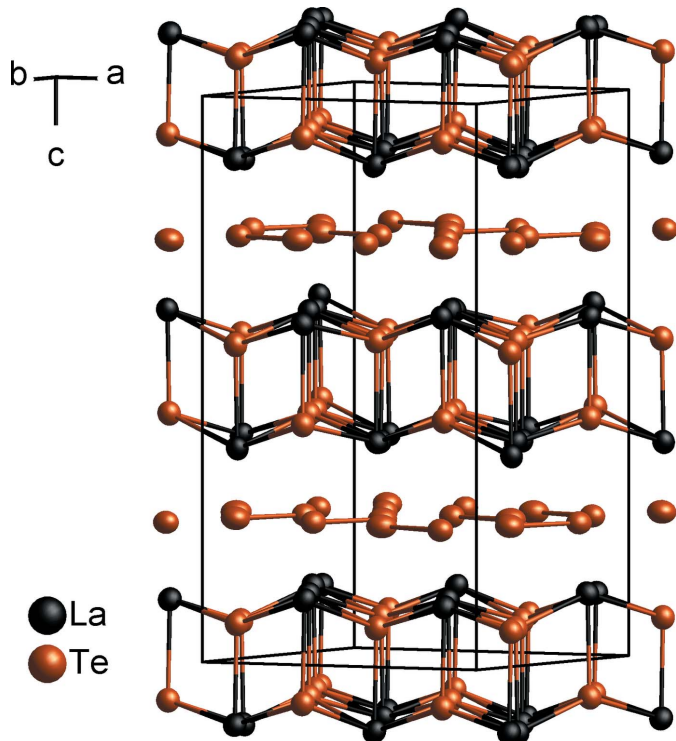


Figure 1

Crystal structure of LaTe_{1.9} with displacement ellipsoids drawn at the 99.95% probability level. The stacking arrangement of puckered [LaTe] slabs and planar [Te] layers along [001] is shown.

from 3.2944(3) to 3.4480(3) between the planar [Te] layer and La. Calculating the bond-valence sum *bvs* (Brese & O'Keeffe, 1991) for each La site results in 2.99 valence units (v.u.) for La1, 3.06 v.u. for La2 and 2.94 v.u. for La3, which are all very close to the expected value of +3 considering the previously discussed charge-balancing situation. The tellurium layer exhibits a pinwheel-like arrangement of four eight-membered Te squares surrounding a single Te²⁻ anion in its centre (Fig. 2), common to all compounds of the CeSe_{1.9} type.

In view of the alternating short and long distances, the Te ring can be understood as being built up from four dinuclear Te₂²⁻ anions enclosing a vacancy with alternating bonding and non-bonding distances of 2.9224(3) and 3.1413(3) Å, respectively.

In accordance with the charge balancing mentioned above and $Z = 20$, a structured formula of LaTe_{1.9} can be written as $[(\text{La}^{3+})_{20}(\text{Te}^{2-})_{20}]$ $[(\text{Te}_2^{2-})_8(\text{Te}^{2-})_2]$. This easily explains the anionic motifs and their quantity in the planar [Te] layer: Te5 and Te6 (both on Wyckoff site 8g) form the dumbbell-shaped Te₂²⁻ anions whereas Te4 (Wyckoff site 2b) represents the isolated Te²⁻ (Fig. 2).

3. Database survey

The CeSe_{1.9} structure type (Plambeck-Fischer *et al.*, 1989) is realized by several rare-earth metal sulfides and selenides but only by a few tellurides, CeTe_{1.9} being one prominent example (Ijjaali & Ibers, 2006). The interatomic distances of LaTe_{1.9} match those observed for CeTe_{1.9} quite well, including the bonding and non-bonding distances in the planar [Te] layers [2.9224(3) Å and 3.1413(3) Å in LaTe_{1.9} vs 2.9194(5) Å and 3.1204(5) Å in CeTe_{1.9}]. However, the bonding Te–Te distances in these two compounds are considerably longer compared to compounds featuring (largely) isolated Te₂²⁻

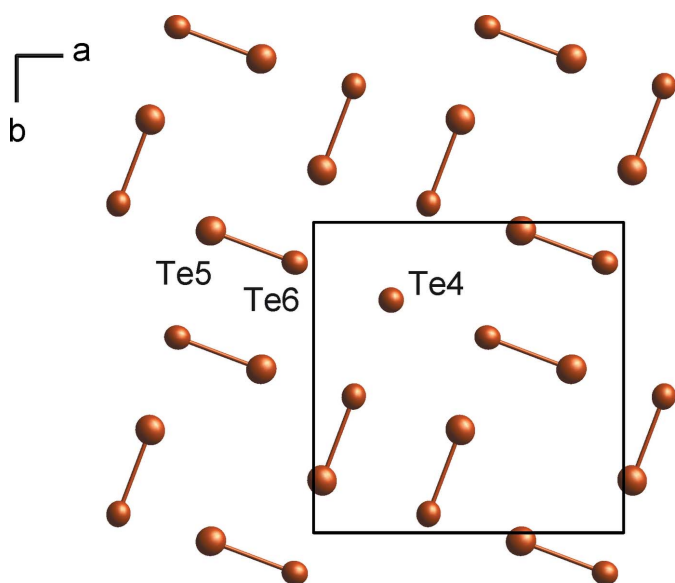


Figure 2

[Te] layer of LaTe_{1.9} with four Te₂²⁻ anions enclosing a vacancy each and surrounding an isolated Te²⁻ anion; displacement ellipsoids are drawn at the 99.95% probability level.

Table 1
Experimental details.

Crystal data	LaTe _{1.90}
Chemical formula	
M_r	381.35
Crystal system, space group	Tetragonal, $P4_3/n$
Temperature (K)	100
a, c (Å)	10.1072 (3), 18.2874 (6)
V (Å ³)	1868.16 (13)
Z	20
Radiation type	Mo $K\alpha$
μ (mm ⁻¹)	25.70
Crystal size (mm)	0.11 × 0.08 × 0.04
Data collection	
Diffractometer	Bruker APEXII CCD
Absorption correction	Multi-scan (<i>TWINABS</i> ; Bruker, 2012)
T_{\min}, T_{\max}	0.399, 0.749
No. of measured, independent and observed [$I > 2\sigma(I)$] reflections	7850, 7850, 5970
R_{int}	0.055
(sin θ/λ) _{max} (Å ⁻¹)	1.000
Refinement	
$R[F^2 > 2\sigma(F^2)], wR(F^2), S$	0.027, 0.061, 1.12
No. of reflections	7850
No. of parameters	69
$\Delta\rho_{\max}, \Delta\rho_{\min}$ (e Å ⁻³)	2.02, -3.08

Computer programs: *APEX2* and *SAINT* (Bruker, 2016), *SHELXT* (Sheldrick, 2015a), *SHELXL* (Sheldrick, 2015b), *DIAMOND* (Brandenburg, 2018) and *publCIF* (Westrip, 2010).

anions as constituting fragments, *e.g.* in α -K₂Te₂ (2.86 Å), β -K₂Te₂ [2.790 (1) Å], Rb₂Te₂ (2.78 Å) or GdTe_{1.8} [2.868 (1) Å] (Böttcher *et al.*, 1993; Poddig *et al.*, 2018).

4. Synthesis and crystallization

Crystals of LaTe_{1.9} were found as a byproduct during the investigation of the system La–Te in chemical transport experiments using iodine as transport agent. All preparation steps were carried out in an argon-filled (5.0, Praxair Deutschland GmbH, Düsseldorf, Germany) glove box (MBraun, Garching, Germany). Starting from the elements, 300 mg of a stoichiometric mixture of La (99.5%, MaTecK) and Te (Merck, > 99.9%, reduced in H₂ stream at 670 K) were ground and loaded into a silica ampule. A small amount of I₂ (Roth, > 99.8%, purified by sublimating twice prior to use) was added inside the glove box before flame-sealing the ampule under dynamic vacuum ($p \leq 1 \times 10^{-3}$ mbar). The ampule was heated with a ramp of 2 K min⁻¹ to 1173 K before applying a gradient from 1173 → 1073 K, where the actual transport took place. After seven days, the ampule was cooled down to room temperature. A synthesis resulting in a phase pure product of LaTe_{1.9} has not yet been successful. The reason is most probably that two other Te-deficient compounds also exist in the composition range LaTe_{2-δ} ($0 \leq \delta \leq 0.2$) along the stoichiometric ditelluride, namely LaTe_{1.94(1)} and LaTe_{1.82(1)} (Poddig & Doert, 2020; Poddig *et al.*, 2020). To address the stability ranges of the individual phases, the chalcogen vapor pressures and temperatures have to be evaluated and controlled precisely during synthesis (Müller *et al.*, 2010).

5. Refinement

Crystal data, data collection and structure refinement details are summarized in Table 1. All investigated crystals of LaTe_{1.9} were found as reticular merohedric twins with a twin index $n = 5$. On a first glance, the diffraction patterns seem to suggest a large tetragonal unit cell with apparent lattice parameters of $a = 22.6211$ (6) Å and $c = 18.3135$ (5) Å, corresponding to a 50-fold superstructure of the basic ZrSSI structure (Fig. 3). Similar apparent supercells have been reported for the sulfides SmS_{1.9} (Tamazyan *et al.*, 2000) or TmS_{1.9} (Müller *et al.*, 2012), and can be explained by twinning along the mirror planes in (100) and (110) of the twin lattice. A schematic scheme drawn along [001] is depicted in Fig. 3, illustrating the lattices of each domain. The corresponding twin law calculated by the diffractometer software (Bruker, 2016) corresponds to the twin law derived for SmS_{1.9} (0.6 –0.8 0 –0.8 –0.6 0 0 0 –1). Both domains were handled during the process of integrating and correcting the data, and the refinements were performed on a HKLF5 format file. The twin ratio of the two domains calculated by *SHELXL* is 0.57 (1):43 (1).

Funding information

Funding for this research was provided by: Deutsche Forschungsgemeinschaft (grant No. Do 560/1).

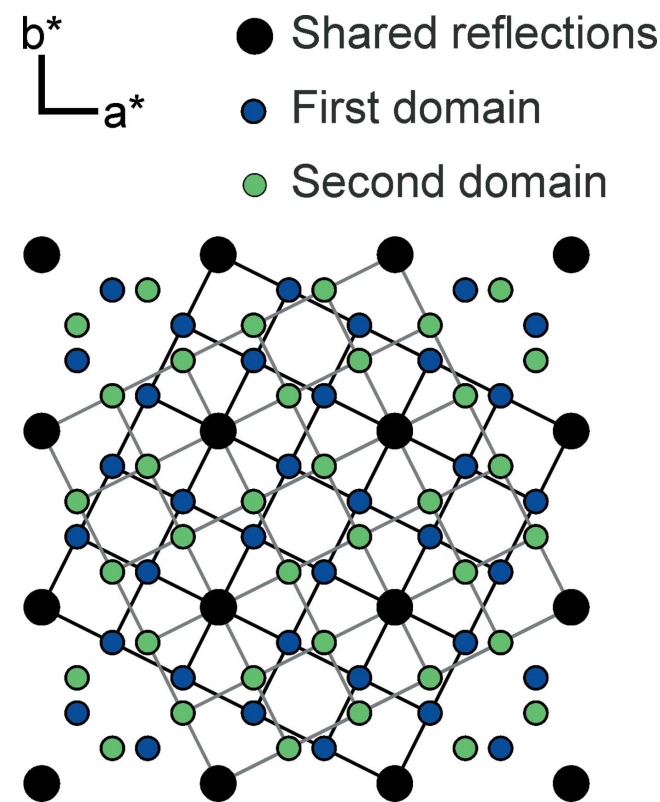


Figure 3

Projection of the X-ray diffraction pattern of a twinned crystal of LaTe_{1.9} along [001]. The individual reflections of the two domains are indicated as green and blue dots, coinciding reflections are marked in black. The axes correspond to the basic structure.

References

- Böttcher, P., Getzschmann, J. & Keller, R. (1993). *Z. Anorg. Allg. Chem.* **619**, 476–488.
- Brandenburg, K. (2018). *DIAMOND*. Crystal Impact GbR, Bonn, Germany.
- Brese, N. E. & O'Keeffe, M. (1991). *Acta Cryst. B* **47**, 192–197.
- Bruker (2012). *TWINABS*. Bruker-AXS, Madison, WI, USA.
- Bruker (2016). *APEX2* and *SAINT*. Bruker AXS, Madison, Wisconsin, USA.
- Doert, T. & Müller, C. J. (2016). *Reference Module in Chemistry, Molecular Sciences and Chemical Engineering*. Amsterdam: Elsevier.
- Ijjaali, I. & Ibers, J. A. (2006). *J. Solid State Chem.* **179**, 3456–3460.
- Klein Haneveld, A. & Jellinek, F. (1964). *Recl Trav. Chim. Pays Bas* **83**, 776–783.
- Müller, C. J., Schwarz, U. & Doert, T. (2012). *Z. Anorg. Allg. Chem.* **638**, 2477–2484.
- Müller, C. J., Schwarz, U., Schmidt, P., Schnelle, W. & Doert, T. (2010). *Z. Anorg. Allg. Chem.* **636**, 947–953.
- Onken, H., Vierheilig, K. & Hahn, H. (1964). *Z. Anorg. Allg. Chem.* **333**, 267–279.
- Plambeck-Fischer, P., Abriel, W. & Urland, W. (1989). *J. Solid State Chem.* **78**, 164–169.
- Poddig, H. & Doert, T. (2020). *Acta Cryst. B* **76**, 1092–1099.
- Poddig, H., Donath, T., Gebauer, P., Finzel, K., Kohout, M., Wu, Y., Schmidt, P. & Doert, T. (2018). *Z. Anorg. Allg. Chem.* **644**, 1886–1896.
- Poddig, H., Finzel, K. & Doert, T. (2020). *Acta Cryst. C* **76**, 530–540.
- Sheldrick, G. M. (2015a). *Acta Cryst. A* **71**, 3–8.
- Sheldrick, G. M. (2015b). *Acta Cryst. C* **71**, 3–8.
- Stöwe, K. (2000a). *J. Solid State Chem.* **149**, 155–166.
- Stöwe, K. (2000b). *J. Alloys Compd.* **307**, 101–110.
- Stöwe, K. (2000c). *Z. Anorg. Allg. Chem.* **626**, 803–811.
- Stöwe, K. (2001). *Z. Kristallogr. Cryst. Mater.* **216**, 215–224.
- Tamazyan, R., Arnold, H., Molchanov, V., Kuzmicheva, G. & Vasileva, I. (2000). *Z. Kristallogr. Cryst. Mater.* **215**, 346–351.
- Westrip, S. P. (2010). *J. Appl. Cryst.* **43**, 920–925.

supporting information

Acta Cryst. (2022). E78, 559–562 [https://doi.org/10.1107/S2056989022004844]

LaTe_{1.9}: a tenfold superstructure of the ZrSSI type

Hagen Poddig and Thomas Doert

Computing details

Data collection: *APEX2* (Bruker, 2016); cell refinement: *SAINT* (Bruker, 2016); data reduction: *SAINT* (Bruker, 2016); program(s) used to solve structure: *SHELXT* (Sheldrick, 2015a); program(s) used to refine structure: *SHELXL* (Sheldrick, 2015b); molecular graphics: *DIAMOND* (Brandenburg, 2018); software used to prepare material for publication: *publCIF* (Westrip, 2010).

Lanthanum telluride (1/1.9)

Crystal data

LaTe _{1.90}	$D_x = 6.779 \text{ Mg m}^{-3}$
$M_r = 381.35$	Mo $K\alpha$ radiation, $\lambda = 0.71073 \text{ \AA}$
Tetragonal, $P4_2/n$	Cell parameters from 9906 reflections
$a = 10.1072 (3) \text{ \AA}$	$\theta = 3.6\text{--}46.4^\circ$
$c = 18.2874 (6) \text{ \AA}$	$\mu = 25.70 \text{ mm}^{-1}$
$V = 1868.16 (13) \text{ \AA}^3$	$T = 100 \text{ K}$
$Z = 20$	Block, black
$F(000) = 3116$	$0.11 \times 0.08 \times 0.04 \text{ mm}$

Data collection

Bruker APEXII CCD	7850 measured reflections
diffractometer	7850 independent reflections
Radiation source: sealed X-ray tube	5970 reflections with $I > 2\sigma(I)$
Graphite monochromator	$R_{\text{int}} = 0.055$
φ and ω scans	$\theta_{\text{max}} = 45.3^\circ, \theta_{\text{min}} = 2.9^\circ$
Absorption correction: multi-scan	$h = -13 \rightarrow 14$
(<i>TWINABS</i> ; Bruker, 2012)	$k = 0 \rightarrow 20$
$T_{\text{min}} = 0.399, T_{\text{max}} = 0.749$	$l = 0 \rightarrow 36$

Refinement

Refinement on F^2	Secondary atom site location: difference Fourier map
Least-squares matrix: full	$w = 1/[\sigma^2(F_o^2) + (0.0122P)^2 + 6.7117P]$
$R[F^2 > 2\sigma(F^2)] = 0.027$	where $P = (F_o^2 + 2F_c^2)/3$
$wR(F^2) = 0.061$	$(\Delta/\sigma)_{\text{max}} = 0.002$
$S = 1.12$	$\Delta\rho_{\text{max}} = 2.02 \text{ e \AA}^{-3}$
7850 reflections	$\Delta\rho_{\text{min}} = -3.08 \text{ e \AA}^{-3}$
69 parameters	Extinction correction: SHELXL-2016/6
0 restraints	(Sheldrick 2015b),
Primary atom site location: iterative	$F_c^* = kFc[1 + 0.001xFc^2\lambda^3/\sin(2\theta)]^{-1/4}$
	Extinction coefficient: 0.001129 (18)

Special details

Geometry. All esds (except the esd in the dihedral angle between two l.s. planes) are estimated using the full covariance matrix. The cell esds are taken into account individually in the estimation of esds in distances, angles and torsion angles; correlations between esds in cell parameters are only used when they are defined by crystal symmetry. An approximate (isotropic) treatment of cell esds is used for estimating esds involving l.s. planes.

Refinement. Refined as a 2-component twin.

Fractional atomic coordinates and isotropic or equivalent isotropic displacement parameters (\AA^2)

	<i>x</i>	<i>y</i>	<i>z</i>	$U_{\text{iso}}^*/U_{\text{eq}}$
La1	0.250000	-0.250000	0.38287 (2)	0.00695 (4)
La2	0.14760 (2)	0.05231 (2)	0.10752 (2)	0.00710 (3)
La3	-0.15137 (2)	-0.04353 (2)	0.38089 (2)	0.00696 (3)
Te1	-0.250000	0.250000	0.43532 (2)	0.00722 (4)
Te2	0.14951 (2)	0.05177 (2)	0.43621 (2)	0.00726 (3)
Te3	-0.15255 (2)	-0.04952 (2)	0.07093 (2)	0.00722 (3)
Te4	-0.250000	-0.250000	0.250000	0.00773 (5)
Te5	-0.02702 (2)	0.16873 (2)	0.25027 (2)	0.00992 (3)
Te6	0.06086 (2)	-0.12938 (2)	0.24930 (2)	0.00770 (3)

Atomic displacement parameters (\AA^2)

	U^{11}	U^{22}	U^{33}	U^{12}	U^{13}	U^{23}
La1	0.00683 (8)	0.00672 (8)	0.00729 (7)	0.00054 (6)	0.000	0.000
La2	0.00723 (6)	0.00691 (6)	0.00715 (5)	0.00000 (5)	0.00005 (4)	0.00083 (4)
La3	0.00657 (6)	0.00689 (6)	0.00744 (5)	0.00015 (5)	-0.00001 (4)	-0.00070 (4)
Te1	0.00701 (9)	0.00696 (9)	0.00769 (8)	0.00009 (7)	0.000	0.000
Te2	0.00684 (7)	0.00726 (7)	0.00767 (5)	-0.00005 (6)	0.00002 (5)	-0.00037 (4)
Te3	0.00712 (7)	0.00697 (7)	0.00756 (5)	0.00007 (6)	0.00001 (5)	0.00005 (5)
Te4	0.00815 (7)	0.00815 (7)	0.00690 (11)	0.000	0.000	0.000
Te5	0.01106 (7)	0.01167 (7)	0.00702 (6)	0.00045 (6)	0.00031 (6)	-0.00005 (5)
Te6	0.00881 (7)	0.00761 (6)	0.00667 (5)	0.00034 (5)	-0.00003 (5)	-0.00016 (5)

Geometric parameters (\AA , $^\circ$)

La1—Te3 ⁱ	3.2938 (2)	La2—Te6	3.2960 (2)
La1—Te3 ⁱⁱ	3.2938 (2)	La2—Te1 ⁱⁱ	3.3198 (2)
La1—Te1 ⁱⁱⁱ	3.3248 (3)	La2—Te5	3.3637 (3)
La1—Te6	3.3329 (3)	La3—Te1	3.2843 (2)
La1—Te6 ^{iv}	3.3329 (2)	La3—Te4	3.3284 (2)
La1—Te2 ^{iv}	3.3593 (2)	La3—Te3 ^{vii}	3.3361 (3)
La1—Te2	3.3594 (2)	La3—Te6	3.3384 (2)
La1—Te5 ⁱⁱ	3.4179 (3)	La3—Te2 ⁱⁱⁱ	3.3460 (2)
La1—Te5 ⁱ	3.4179 (3)	La3—Te2	3.3465 (3)
La2—Te3 ^v	3.2637 (2)	La3—Te3 ⁱⁱ	3.3574 (3)
La2—Te2 ^{vi}	3.2649 (3)	La3—Te6 ^{vii}	3.4194 (3)
La2—Te3	3.2726 (3)	La3—Te5	3.4480 (3)
La2—Te2 ⁱ	3.2920 (3)	Te5—Te6 ^{vi}	2.9224 (3)

La2—Te5 ⁱ	3.2944 (3)	Te5—Te6	3.1413 (3)
Te3 ⁱ —La1—Te3 ⁱⁱ	150.272 (10)	Te2 ⁱⁱⁱ —La3—Te3 ⁱⁱ	73.330 (5)
Te3 ⁱ —La1—Te1 ⁱⁱⁱ	75.136 (5)	Te2—La3—Te3 ⁱⁱ	84.571 (6)
Te3 ⁱⁱ —La1—Te1 ⁱⁱⁱ	75.136 (5)	Te1—La3—Te6 ^{vii}	74.669 (6)
Te3 ⁱ —La1—Te6	127.287 (6)	Te4—La3—Te6 ^{vii}	59.908 (4)
Te3 ⁱⁱ —La1—Te6	76.715 (5)	Te3 ^{vii} —La3—Te6 ^{vii}	72.455 (5)
Te1 ⁱⁱⁱ —La1—Te6	137.132 (4)	Te6—La3—Te6 ^{vii}	89.696 (6)
Te3 ⁱ —La1—Te6 ^{iv}	76.715 (5)	Te2 ⁱⁱⁱ —La3—Te6 ^{vii}	135.020 (7)
Te3 ⁱⁱ —La1—Te6 ^{iv}	127.288 (6)	Te2—La3—Te6 ^{vii}	135.283 (7)
Te1 ⁱⁱⁱ —La1—Te6 ^{iv}	137.132 (4)	Te3 ⁱⁱ —La3—Te6 ^{vii}	131.586 (6)
Te6—La1—Te6 ^{iv}	85.735 (8)	Te1—La3—Te5	76.027 (6)
Te3 ⁱ —La1—Te2 ^{iv}	85.364 (5)	Te4—La3—Te5	90.060 (6)
Te3 ⁱⁱ —La1—Te2 ^{iv}	86.094 (5)	Te3 ^{vii} —La3—Te5	135.955 (7)
Te1 ⁱⁱⁱ —La1—Te2 ^{iv}	73.124 (5)	Te6—La3—Te5	55.118 (5)
Te6—La1—Te2 ^{iv}	135.915 (6)	Te2 ⁱⁱⁱ —La3—Te5	134.911 (7)
Te6 ^{iv} —La1—Te2 ^{iv}	72.977 (5)	Te2—La3—Te5	72.489 (5)
Te3 ⁱ —La1—Te2	86.094 (5)	Te3 ⁱⁱ —La3—Te5	129.745 (6)
Te3 ⁱⁱ —La1—Te2	85.363 (5)	Te6 ^{vii} —La3—Te5	64.015 (6)
Te1 ⁱⁱⁱ —La1—Te2	73.123 (5)	La3—Te1—La3 ^{viii}	144.714 (11)
Te6—La1—Te2	72.977 (5)	La3—Te1—La2 ^{vii}	85.769 (5)
Te6 ^{iv} —La1—Te2	135.915 (6)	La3 ^{viii} —Te1—La2 ^{vii}	86.028 (4)
Te2 ^{iv} —La1—Te2	146.246 (10)	La3—Te1—La2 ^{vi}	86.029 (4)
Te3 ⁱ —La1—Te5 ⁱⁱ	126.928 (6)	La3 ^{viii} —Te1—La2 ^{vi}	85.769 (4)
Te3 ⁱⁱ —La1—Te5 ⁱⁱ	76.389 (5)	La2 ^{vii} —Te1—La2 ^{vi}	152.703 (10)
Te1 ⁱⁱⁱ —La1—Te5 ⁱⁱ	135.428 (4)	La3—Te1—La1 ⁱⁱⁱ	107.643 (5)
Te6—La1—Te5 ⁱⁱ	65.244 (6)	La3 ^{viii} —Te1—La1 ⁱⁱⁱ	107.643 (5)
Te6 ^{iv} —La1—Te5 ⁱⁱ	51.284 (5)	La2 ^{vii} —Te1—La1 ⁱⁱⁱ	103.648 (5)
Te2 ^{iv} —La1—Te5 ⁱⁱ	71.386 (5)	La2 ^{vi} —Te1—La1 ⁱⁱⁱ	103.648 (5)
Te2—La1—Te5 ⁱⁱ	137.123 (7)	La2 ⁱ —Te2—La2 ^{vi}	86.685 (6)
Te3 ⁱ —La1—Te5 ⁱ	76.389 (5)	La2 ⁱ —Te2—La3 ⁱⁱⁱ	104.300 (6)
Te3 ⁱⁱ —La1—Te5 ⁱ	126.928 (6)	La2 ^{vi} —Te2—La3 ⁱⁱⁱ	105.511 (6)
Te1 ⁱⁱⁱ —La1—Te5 ⁱ	135.428 (4)	La2 ⁱ —Te2—La3	148.230 (7)
Te6—La1—Te5 ⁱ	51.283 (5)	La2 ^{vi} —Te2—La3	85.472 (6)
Te6 ^{iv} —La1—Te5 ⁱ	65.243 (6)	La3 ⁱⁱⁱ —Te2—La3	107.465 (6)
Te2 ^{iv} —La1—Te5 ⁱ	137.122 (7)	La2 ⁱ —Te2—La1	85.364 (5)
Te2—La1—Te5 ⁱ	71.387 (5)	La2 ^{vi} —Te2—La1	149.063 (7)
Te5 ⁱⁱ —La1—Te5 ⁱ	89.144 (9)	La3 ⁱⁱⁱ —Te2—La1	105.424 (7)
Te3 ^v —La2—Te2 ^{vi}	76.566 (5)	La3—Te2—La1	85.737 (5)
Te3 ^v —La2—Te3	78.875 (7)	La2 ^v —Te3—La2	101.125 (7)
Te2 ^{vi} —La2—Te3	88.008 (6)	La2 ^v —Te3—La1 ^{vi}	105.604 (7)
Te3 ^v —La2—Te2 ⁱ	75.263 (5)	La2—Te3—La1 ^{vi}	86.313 (5)
Te2 ^{vi} —La2—Te2 ⁱ	86.496 (6)	La2 ^v —Te3—La3 ⁱⁱ	104.549 (6)
Te3—La2—Te2 ⁱ	154.134 (7)	La2—Te3—La3 ⁱⁱ	85.690 (6)
Te3 ^v —La2—Te5 ⁱ	141.133 (7)	La1 ^{vi} —Te3—La3 ⁱⁱ	149.757 (7)
Te2 ^{vi} —La2—Te5 ⁱ	125.814 (7)	La2 ^v —Te3—La3 ^{vii}	105.889 (6)
Te3—La2—Te5 ⁱ	127.388 (7)	La2—Te3—La3 ^{vii}	152.986 (8)
Te2 ⁱ —La2—Te5 ⁱ	75.182 (6)	La1 ^{vi} —Te3—La3 ^{vii}	86.610 (5)

Te3 ^v —La2—Te6	141.795 (7)	La3 ⁱⁱ —Te3—La3 ^{vii}	87.422 (6)
Te2 ^{vi} —La2—Te6	128.902 (6)	La3 ^{vii} —Te4—La3 ⁱⁱ	88.029 (7)
Te3—La2—Te6	74.873 (6)	La3 ^{vii} —Te4—La3 ^{ix}	121.144 (4)
Te2 ⁱ —La2—Te6	127.073 (7)	La3 ⁱⁱ —Te4—La3 ^{ix}	121.144 (4)
Te5 ⁱ —La2—Te6	52.645 (6)	La3 ^{vii} —Te4—La3	121.144 (4)
Te3 ^v —La2—Te1 ⁱⁱ	75.603 (6)	La3 ⁱⁱ —Te4—La3	121.145 (4)
Te2 ^{vi} —La2—Te1 ⁱⁱ	152.164 (7)	La3 ^{ix} —Te4—La3	88.029 (7)
Te3—La2—Te1 ⁱⁱ	87.208 (5)	Te6 ^{vi} —Te5—Te6	175.690 (9)
Te2 ⁱ —La2—Te1 ⁱⁱ	85.964 (5)	Te6 ^{vi} —Te5—La2 ^{vi}	63.706 (6)
Te5 ⁱ —La2—Te1 ⁱⁱ	77.677 (6)	Te6—Te5—La2 ^{vi}	118.432 (7)
Te6—La2—Te1 ⁱⁱ	75.863 (6)	Te6 ^{vi} —Te5—La2	120.999 (8)
Te3 ^v —La2—Te5	141.908 (8)	Te6—Te5—La2	60.772 (5)
Te2 ^{vi} —La2—Te5	73.230 (6)	La2 ^{vi} —Te5—La2	133.008 (9)
Te3—La2—Te5	77.427 (6)	Te6 ^{vi} —Te5—La1 ^{vi}	62.856 (5)
Te2 ⁱ —La2—Te5	124.638 (7)	Te6—Te5—La1 ^{vi}	114.389 (7)
Te5 ⁱ —La2—Te5	76.593 (7)	La2 ^{vi} —Te5—La1 ^{vi}	125.977 (7)
Te6—La2—Te5	56.276 (6)	La2—Te5—La1 ^{vi}	82.945 (6)
Te1 ⁱⁱ —La2—Te5	131.965 (7)	Te6 ^{vi} —Te5—La3	116.808 (7)
Te1—La3—Te4	133.902 (7)	Te6—Te5—La3	60.669 (5)
Te1—La3—Te3 ^{vii}	86.745 (5)	La2 ^{vi} —Te5—La3	83.822 (6)
Te4—La3—Te3 ^{vii}	73.231 (5)	La2—Te5—La3	120.748 (7)
Te1—La3—Te6	130.412 (7)	La1 ^{vi} —Te5—La3	113.748 (7)
Te4—La3—Te6	60.731 (4)	Te5 ⁱ —Te6—Te5	85.692 (9)
Te3 ^{vii} —La3—Te6	133.378 (6)	Te5 ⁱ —Te6—La2	63.650 (6)
Te1—La3—Te2 ⁱⁱⁱ	73.811 (6)	Te5—Te6—La2	62.951 (6)
Te4—La3—Te2 ⁱⁱⁱ	134.830 (7)	Te5 ⁱ —Te6—La1	65.861 (5)
Te3 ^{vii} —La3—Te2 ⁱⁱⁱ	74.503 (5)	Te5—Te6—La1	120.592 (7)
Te6—La3—Te2 ⁱⁱⁱ	135.279 (7)	La2—Te6—La1	128.888 (7)
Te1—La3—Te2	85.654 (5)	Te5 ⁱ —Te6—La3	120.461 (7)
Te4—La3—Te2	132.068 (6)	Te5—Te6—La3	64.213 (5)
Te3 ^{vii} —La3—Te2	147.001 (7)	La2—Te6—La3	126.382 (7)
Te6—La3—Te2	73.072 (6)	La1—Te6—La3	86.290 (6)
Te2 ⁱⁱⁱ —La3—Te2	72.535 (6)	Te5 ⁱ —Te6—La3 ⁱⁱ	121.325 (7)
Te1—La3—Te3 ⁱⁱ	147.141 (7)	Te5—Te6—La3 ⁱⁱ	122.568 (7)
Te4—La3—Te3 ⁱⁱ	72.959 (5)	La2—Te6—La3 ⁱⁱ	83.998 (6)
Te3 ^{vii} —La3—Te3 ⁱⁱ	84.626 (6)	La1—Te6—La3 ⁱⁱ	116.758 (7)
Te6—La3—Te3 ⁱⁱ	75.783 (6)	La3—Te6—La3 ⁱⁱ	118.169 (7)

Symmetry codes: (i) $-y+1/2, x, -z+1/2$; (ii) $y, -x-1/2, -z+1/2$; (iii) $-x, -y, -z+1$; (iv) $-x+1/2, -y-1/2, z$; (v) $-x, -y, -z$; (vi) $y, -x+1/2, -z+1/2$; (vii) $-y-1/2, x, -z+1/2$; (viii) $-x-1/2, -y+1/2, z$; (ix) $-x-1/2, -y-1/2, z$.